

# Stem cell derived neurosphere assay highlights the effects of infection on human cortical development

**Edward Drydale**

University of Oxford

**Phalguni Rath**

University of Oxford

**Katie Holden**

University of Oxford

**Thomas Johnson**

University of Oxford

**James Bancroft**

University of Oxford

**Lahiru Handunnetthi** (✉ [lahiru@well.ox.ac.uk](mailto:lahiru@well.ox.ac.uk))

University of Oxford <https://orcid.org/0000-0002-8242-3722>

---

## Article

### Keywords:

**Posted Date:** October 25th, 2022

**DOI:** <https://doi.org/10.21203/rs.3.rs-2184467/v1>

**License:**   This work is licensed under a Creative Commons Attribution 4.0 International License.

[Read Full License](#)

---

# Abstract

Defective cortical development is responsible for neurodevelopmental disorders that manifest in childhood and adolescence. However, model systems that can explore the effects of genetic and environmental factors on human cortical development are not well established. Therefore, we developed a novel neurosphere assay that combined recent progress in induced pluripotent stem cell (iPSC) differentiation with advanced live cell imaging techniques to study key aspects of human cortical development. We subsequently applied this assay to investigate the effects of viral infection on cortical development given its established link to neurodevelopmental disorders. We found that viral infection substantially restricted both radial glia growth and neural cell migration. These findings provide new insight into how infections exert deleterious effects on the developing cortex and thus carry important implications for future disease prevention strategies.

## Introduction

The cerebral cortex is responsible for higher cognitive function in humans. It is a laminated structure that contains a bewildering diversity of neurons and complex networks of connections. Intriguingly, these cortical cells can be traced back to just a few neuronal progenitors at the start of cortical neurogenesis<sup>1</sup>. Through a set of tightly coordinated events, these neuronal progenitors undergo proliferation, migration, differentiation, and functional integration into neuronal circuitry<sup>1</sup>. Defects in cortical development are thought to contribute to neurodevelopmental disorders that affect more than 4% of children and adolescents worldwide<sup>2</sup>. This is further supported by studies that link genetic risk factors in autism and schizophrenia to cortical developmental processes<sup>3,4</sup>. There is therefore a need to better understand mechanisms that govern human cortical development in health and in disease.

The human cortical development is astonishingly complex<sup>1</sup>. At the start, neuroepithelial cells transform into radial glia cells, establishing the ventricular zone. The ventricular radial glia cells not only undergo self-renewal but also produce nascent neurons. These neurons then migrate along the radial fibres of ventricular glia to create the deep layers of the cortex. In parallel, the ventricular radial glia cells generate intermediate progenitor cells and outer radial glial cells that migrate into the expanded outer subventricular zone in humans. The outer radial glia cells subsequently become the predominant source of neurons that create the upper layers of the cortex<sup>5</sup>. Unsurprisingly, these developmental processes are vulnerable to environmental influences. In line with this notion, studies suggest that inflammatory insults such as viral infections can influence cortical development and increase the risk of neurodevelopmental disorders<sup>6,7</sup>.

Therefore, modelling aspects of cortical development is a key research goal in neurodevelopmental disorders. However, this has been difficult to achieve for several reasons. First, previous studies have focused on rodent models<sup>8</sup> but human cortical development differs from that of rodents. For example, the outer radial glia population is largely missing in mouse brains, but these cells form an essential part

of human cortical development<sup>5</sup>. Second, neural cell migration is a highly dynamic process making it difficult to visualise over time. As a result, previous studies have analysed only a few time points in fixed samples, providing poor temporal resolution<sup>9, 10</sup>. To address these challenges, first we developed a novel neurosphere assay by combining recent advances in human iPSC differentiation with live cell imaging techniques. Second, we created an automated pipeline for high throughput image analysis. Finally, we applied this neurosphere assay to investigate how viral infections could influence cortical developmental processes.

## Results

### IPSC derived neuronal progenitors of cortical lineage

We differentiated human iPSCs into neuronal progenitors and cortical neurons using previously established methodology<sup>11</sup>. The differentiated neural cells were characterised using immunofluorescence. First, we demonstrated that our iPSC lines retained pluripotency through the expression of *OCT4* and *NANOG* (*supplementary figures 1 and 2*). Second, we confirmed the appearance of primary and intermediate neuronal progenitor cells using *PAX6* and *TBR2* respectively (*figure 1a and 1b*). Third, we demonstrated that these neuronal progenitor cells gave rise to both *CTIP2*-expressing deep cortical neurons and *BRN2*-expressing upper-layer cortical neurons (*figure 1c-1f*).

### Figure 1

Figure 1: iPSC derived cortical lineage neuronal progenitor cells and cortical neurons. A: *PAX6* expressing primary neuronal progenitors. B: *TBR2* expressing intermediate neuronal progenitor cells. C and D: *CTIP2* expressing deep cortical layer neurons. D and E: *BRN2* expressing upper-layer cortical neurons.

We used neuronal progenitor cells from day twenty-five of differentiation to make neurospheres. The neuronal progenitor cells were first dissociated into single cells and subsequently allowed to reaggregate in 96-well V-bottom plates coated with non-adhesive compounds. This resulted in the formation of three dimensional neurospheres that were transferred onto a matrigel matrix after 24 hours. We characterised the neurospheres using immunofluorescence to confirm the presence of intermediate progenitor cells and cortical neurons (*figure 2*). Over time, we observed the evolution of neurospheres (*figure 2a and 2b*). Specifically, we found an increasing number of *TBR2* expressing intermediate progenitor cells appearing over time (*figure 2b*). Similarly, an increasing number of nascent *CTIP2* expressing cortical neurons migrated along the radial fibres over time (*figure 2a*).

## Figure 2

Figure 2: Evolution of neurospheres over three time points 6-, 12-, and 24-hours using immunofluorescence. Top panel: Appearance of CTIP2 expressing deep cortical layer neurons over time. 3X and 14X zoom panels show the migration and differentiation of CTIP2 expressing neurons as they reach the outer edge of neurospheres. Bottom panel: Appearance of TBR2 expressing intermediate neuronal progenitor cells over time. 3X and 14X zoom panels show the appearance of TBR2 expressing intermediate neuronal progenitors within the radial extensions of neurospheres over time.

### Live cell imaging of neurospheres and automated analysis

Time-lapse images of neurospheres were acquired using fluorogenic live cell probes. We used SiR-tubulin, a highly specific marker of microtubules, to identify radial glia fibres. Whereas SPY555-DNA, a highly specific DNA probe, was used to identify the nuclei of migrating neural cells. Images were taken every 30 minutes over a period of 48 hours using SpinSR microscope system (Olympus). A total depth of 140um was imaged in the z-plane at 10um intervals using a 10x objective. We captured the growth of radial fibres away from the central mass of cells (*figure 3, bottom panel*) and migration of neural cells along the radial fibres (*figure 3, middle panel*) (*supplementary movie 1*).

## Figure 3

Figure 3: Evolution of a single neurosphere over time using live cell imaging. The top panel shows combined radial glia (Tubulin) and nuclei of migrating neural cells (DNA) at four selected time points 0, 12, 24, 36 and 48 hours. The middle and bottom panels show the breakdown of nuclei of migrating neural cells (DNA) and radial glia (Tubulin) respectively at 0, 12, 24, 36 and 48 hours. The middle and bottom panels show the breakdown of nuclei of migrating neural cells and radial glia respectively at time points 0, 12, 24, 36 and 48 hours.

To robustly quantify the dynamic nature of neurospheres over time, we developed an automated pipeline for image analysis using the Arivis Vision4D image analysis platform. The projected images were processed using closing and blurring algorithms. An intensity threshold was then applied to define areas of migrating neural cells and radial fibre extensions using nuclear and tubulin staining respectively (*figure 4 and supplementary movies 2 and 3*) Finally, radial fibre and neural cell migration areas were calculated

after each time point. At 48 hours, the average radial fibre area was  $4.3\text{mm}^2$  (SEM:  $0.74\text{mm}^2$ ) whereas the neural migration area was  $1.78\text{mm}^2$  (SEM:  $0.09\text{mm}^2$ ).

#### Figure 4:

Figure 4: Automated analysis pipeline. Top panel shows the temporal evolution of a single neurosphere. The middle panel shows how the area of migrating neural cells is tracked over time. The bottom panel shows how the area of radial glia growth is quantified over time.

#### Effects of viral infection on cortical development

Given the emerging role of *in utero* viral infections in schizophrenia and autism<sup>12,13</sup>, we investigated the effects of viral infection on radial glia growth and neural cell migration using our neurosphere assay. We used polyinosinic:polycytidylic acid (polyI:C), a well-established viral mimic, to recapitulate infection twelve hours prior to live imaging. The neurospheres were constructed and live imaging was carried out over a period of 48 hours as described above. The areas encompassing radial fibres and migrating neural cells were calculated using the automated pipeline. Linear mixed effects model showed that radial glia growth was greater in unstimulated neurospheres relative to stimulated neurospheres by  $0.028\text{mm}^2/\text{hour}$  (SE: $0.0046\text{mm}^2/\text{hour}$ ,  $p=1.78\text{e-}05$ ) (figure 5d). A likelihood-ratio test indicated that a model that included the interaction between time and stimulation status (i.e. allowing different rates of growth based on stimulation status) was better fit for radial glial growth data ( $\chi^2 = 18.9$ ,  $p=1.33\text{e-}05$ ). Also, linear mixed effects model identified that neural cell migration was greater in unstimulated neurospheres by  $0.011\text{mm}^2/\text{hour}$  (SE: $0.0025\text{mm}^2/\text{hour}$ ,  $P=0.0009$ ) (figure 5e). Similarly, a model that included the interaction between time and stimulation status (i.e. allowing different rates of growth based on stimulation status) was a better fit for neural migration data ( $\chi^2 = 11.5$ ,  $p=0.0007$ ). Furthermore, we replicated the effects of polyI:C on radial glia extension and neural migration using immunofluorescence data. Similar to our findings from live cell imaging, we found that polyI:C stimulation resulted in significant reductions in radial glia growth ( $p=0.0069$ ) and neural migration ( $p=0.0033$ ) at 24 hours (figure 5b and 5c).

#### Figure 5:

Figure 5: The effect of viral infection on cortical development. A: Images of fixed polyI:C stimulated and unstimulated neurospheres after 24 hours. B and C: Analysis of immunofluorescence data from fixed

neurospheres B: Comparison of radial fibre extension between polyI:C stimulated and unstimulated neurospheres using immunofluorescence. C: Comparison of neural migration area between polyI:C stimulated and unstimulated neurospheres using immunofluorescence. D and E: Analysis of live imaging data. D: Mixed effects linear models showing neural migration based on stimulation status over time. E: Mixed effects linear models showing radial glia extension based on stimulation status over time.

## Discussion

The iPSC derived neurospheres combined with state-of-the-art live cell imaging and analysis represent a novel assay to study human radial glia extension and neural cell migration during cortical development. This is a substantial step forward in modelling aspects of human cortical development and overcomes limitations linked to rodent models<sup>8</sup>. We demonstrated the cortical identity of these neurospheres through the appearance of cortical lineage neuronal progenitors as well as cortical layer specific neurons. A key feature of our work was the accompanying automated pipeline that not only facilitated high throughput image analysis but also eliminated investigator bias linked to manual analysis techniques. Importantly, this neurosphere assay offers a unique platform to study the effects of genetic and environmental factors linked to neurodevelopmental disorders in future research.

We highlighted the utility of this neurosphere assay by investigating how viral infection could influence radial glia extension and neural cell migration. Interestingly, we found that polyI:C, a viral infection mimic, substantially reduced both radial glia growth and neural cell migration over time. These findings were further supported by immunofluorescence experiments that demonstrated polyI:C stimulation led to reduced growth of radial glia fibres and neural cell migration in fixed neurospheres. Given that the radial glia extensions provide scaffolding for nascent neurons to migrate towards their cortical destination, our findings for the first time demonstrate how viral infections could exert deleterious effects on the developing human cortex. These findings are in line with epidemiological studies that show that maternal infections during pregnancy increase the risk of neurodevelopmental disorders in the offspring<sup>12, 13</sup>, and previous observations that iPSC derived neuronal progenitors from schizophrenia patients display reduced migratory ability<sup>9</sup>.

This study has several key strengths. The neuronal progenitors are derived from human iPSCs and thus provide insight into the unique cortical development in humans. Also, this is the first-time non-toxic live imaging probes have been used to study neural migration, providing valuable temporal insight into these dynamic processes that were not previously captured. Lastly, our automated analysis pipeline makes this assay high throughput and eliminates the potential for investigator bias. There were also limitations to this study. First, this in vitro assay cannot fully capture the complexity of the in vivo environment necessary for successful neuronal progenitor cell migration. Second, although an established viral mimic, polyI:C cannot fully recapitulate the effect of viral infection during cortical development.

In conclusion, we developed a highly novel neurosphere assay to better understand key aspects of human cortical development. We combined advances in iPSC differentiation with live cell imaging techniques to

shed light on the dynamic process of radial glia growth and neural cell migration. We envisage this neurosphere assay will be a key scientific resource for modelling neurodevelopmental disorders in the future. To highlight this utility, we demonstrated that viral infection could reduce both radial glia growth and neural cell migration. These findings carry implications for future prevention strategies of neurodevelopmental disorders.

## Methods

### IPSC differentiation and neurosphere formation

HPSI0114i-Kolf\_2 human induced pluripotent stem cells were purchased from the Wellcome Sanger Institute (Biosample: SAMEA2547615) and maintained in Essential 8 medium (Thermo Fisher Scientific A1517001) on Vitronectin (Thermo Fisher Scientific CTS279S3) coated tissue culture dishes. The pluripotency of these iPSCs was established based on the expression of OCT4 and NANOG using immunofluorescence and Fluorescence Activated Cell Sorting (FACS) (*supplementary figures 1 and 2*). Subsequently, the iPSCs were differentiated into neuronal progenitor cells and cortical neurons as described previously<sup>11</sup>. Briefly, neuronal induction was carried out using 1 $\mu$ M Dorsomorphin (Bio-Techne, 3093/10) and 10  $\mu$ M SB431542 (Tocris Bioscience, 1614) in neuronal maintenance medium (NMM) (*supplementary table 1*). The appearance of a neuroepithelial sheet was noted after 8-12 days. At this point, the neuroepithelial cells were dissociated using 2 mg/mL Dispase II (Gibco™ 17105041) and replated on growth factor reduced matrigel coated plates. Upon appearance of neural rosettes, the cells were maintained in 20 ng/mL FGF2-supplemented NMM for 4 to 5 days.

On day 25, the cells were dissociated into single cells using Accutase (Gibco™ A1110501) and subsequently reaggregated in 96-well V-bottom plates to form three dimensional neurospheres. Each neurosphere contained approximately 10,000 neuronal progenitors. The experimental condition underwent polyI:C (100 $\mu$ g/ml) stimulation 12 hours prior to live cell imaging. After 24 hours, the neurospheres were transferred to a 24 well plate coated with GFR matrigel (Corning, 354230) for live imaging. The cortical identity of neurospheres was checked based on the appearance of PAX6 expressing primary neuronal progenitors and TBR2 expressing intermediate neuronal progenitors (figure 2a and 2b). In parallel, a proportion of neuronal progenitors were further differentiated in 2D culture to confirm the appearance of cortical neurons. After 90 days in culture, the presence of both CTIP2 expressing deep layer and BRN2 expressing upper layer neurons were confirmed using immunofluorescence (figure 2c and 2f)

### Live image acquisition and analysis pipeline

For live cell imaging, neurospheres grown in 24-well optical bottomed plates (Ibidi 82426) were incubated with SiR-Tubulin and SPY-555-DNA at 100 nM concentration 2 hours prior to imaging. All images were acquired using an Olympus IXplore Spin-SR, using a 50  $\mu$ m pinhole confocal spinning disk and a

Hamamatsu ORCA Fusion BT camera. 140  $\mu\text{m}$  z-stacks with a z spacing of 10  $\mu\text{m}$  were taken every 30 minutes over a total time course of 48 hours. These stacks were captured as tiled regions using a 10x, 0.4 NA air Objective lens. See *supplementary table 3* for individual channel and filter details. Live cell migration analysis was performed using a pipeline created in Arivis AG, Germany ([www.arivis.com](http://www.arivis.com)). First, maximum projections were generated from the image z-stacks. The projected (max-intensity) images were then processed to smooth the channels using closing and blurring algorithms. An intensity threshold was then applied to define the migrating progenitor cells using nuclear staining and radial fibre regions based on tubulin staining. Further filtering to segments was applied based on size to exclude small artifacts, after which the area was calculated at each timepoint.

## Immunofluorescence

Cells grown on 24 well plates (Ibidi 82426) were fixed in 4% paraformaldehyde for 15 mins. The cells were permeabilized using 0.1% Triton-X100 in PBS and blocked for 1 hour with 5% fish gelatin and 0.3M glycine in PBS. Subsequently, the cells were stained with primary antibodies to OCT4 (Cell Signaling Technology, 75463S), NANOG (Cell Signaling Technology, 3580S), PAX6 (Cell Signaling Technology, 60433), TBR2 (Cell Signaling Technology, 81493), CTIP2 (Cell Signaling Technology, 12120), BRN2 (Cell Signaling Technology, 12137), Nestin (Cell Signaling Technology, 33475), and TUJ1 (Cell Signaling Technology 4466) diluted in blocking solution at 4°C overnight. The cells were washed and incubated with secondary antibodies (Goat anti-Mouse IgG Alexa Fluor™ 488, Invitrogen A11029, Goat anti-Rabbit IgG, Alexa Fluor™ 568, Invitrogen A11036) diluted 1:1000 in PBS, for 1 hour at room temperature. Also, the cells were stained with 1  $\mu\text{M}$  DAPI. Images were acquired using an Olympus IXplore Spin-SR, using a 50  $\mu\text{m}$  pinhole confocal spinning disk and a Hamamatsu ORCA Fusion BT camera. 50  $\mu\text{m}$  z-stacks with a z spacing of 2  $\mu\text{m}$  were captured as tiled regions using a 20x, 0.8 NA air objective lens. See *supplementary table 4* for individual channel and filter details.

## Statistical analysis

The '*lmer4*' package in R was used to assess the relationship between time and two separate outcomes of interest in this study, 1) radial glia growth and 2) neural migration. The neurospheres were either unstimulated or stimulated with polyI:C. The following two linear mixed effects models were used to explore the association between time and individual outcomes:

*Model 1: Outcome ~ Time + Stimulation Status (1+ Time|Neurospheres)*

*Model 2: Outcome ~ Time  $\times$  Stimulation Status (1+ Time|Neurospheres)*

The first model included one fixed effects parameter, status of stimulation with Poly:IC. This modelled two regression lines (stimulated vs. unstimulated) that have different starting points (i.e. intercepts) but



the same rate of change in outcome (i.e. identical slopes). The second model included another fixed effects parameter, an interaction term between status of stimulation and time. This modelled two regression lines (stimulated vs. unstimulated) that have different starting points (i.e., intercepts) and different rates of change in outcome (i.e. different slopes). Both models included the following random effects parameters: 1) each neurosphere sample (i.e. random intercepts) and 2) average change in outcome per unit time for each neurosphere sample (i.e. random slopes). A likelihood ratio test was carried out to identify the model with a better fit to the data. In parallel, radial glia growth and neural migration areas in fixed neurosphere were compared between stimulated and unstimulated conditions using a two-tailed t-test and a significance threshold of 0.05.

## **Declarations**

### **Acknowledgments**

This work was supported by National Institute for Health Research U.K. and John Fell Fund from the University of Oxford. This work was further supported by Wellcome Trust Grants (090532/Z/09/Z and 203141/Z/16/Z) to core facilities Wellcome Centre for Human Genetics, and the Oxford Biomedical Research Computing (BMRC) facility. The authors would like to thank ARIVIS for their support in developing the pipelines used for image analysis.

### **Data Availability**

The data that support the findings of this study are available from the corresponding author upon reasonable request.

### **Author contributions**

ED: Methodology, Formal analysis, Investigation, Writing - Review & Editing; PR: Methodology, Investigation, Writing - Review & Editing; KH: Methodology, Investigation, Writing - Review & Editing; TJ: Methodology, Formal analysis, Writing - Review & Editing; JB: Conceptualization, Methodology, Resources, Writing - Review & Editing, Supervision; LH: Conceptualization, Methodology, Resources, Writing - Original Draft, Writing - Review & Editing, Supervision, Funding acquisition.

### **Declaration of competing interests**

All other authors declare no competing interests.

## References

1. Miller DJ, Bhaduri A, Sestan N, Kriegstein A. Shared and derived features of cellular diversity in the human cerebral cortex. *Curr Opin Neurobiol* **56**, 117–124 (2019).
2. Frances L, *et al.* Current state of knowledge on the prevalence of neurodevelopmental disorders in childhood according to the DSM-5: a systematic review in accordance with the PRISMA criteria. *Child Adolesc Psychiatry Ment Health* **16**, 27 (2022).
3. Gulsuner S, *et al.* Spatial and temporal mapping of de novo mutations in schizophrenia to a fetal prefrontal cortical network. *Cell* **154**, 518–529 (2013).
4. Satterstrom FK, *et al.* Large-Scale Exome Sequencing Study Implicates Both Developmental and Functional Changes in the Neurobiology of Autism. *Cell* **180**, 568–584 e523 (2020).
5. Hansen DV, Lui JH, Parker PR, Kriegstein AR. Neurogenic radial glia in the outer subventricular zone of human neocortex. *Nature* **464**, 554–561 (2010).
6. Warre-Cornish K, *et al.* Interferon-gamma signaling in human iPSC-derived neurons recapitulates neurodevelopmental disorder phenotypes. *Sci Adv* **6**, eaay9506 (2020).
7. Handunnetthi L, Saatci D, Hamley JC, Knight JC. Maternal immune activation downregulates schizophrenia genes in the foetal mouse brain. *Brain Commun* **3**, fcab275 (2021).
8. Ducker M, Millar V, Ebner D, Szele FG. A Semi-automated and Scalable 3D Spheroid Assay to Study Neuroblast Migration. *Stem Cell Reports* **15**, 789–802 (2020).
9. Brennand K, *et al.* Phenotypic differences in hiPSC NPCs derived from patients with schizophrenia. *Mol Psychiatry* **20**, 361–368 (2015).
10. Delaloy C, *et al.* MicroRNA-9 coordinates proliferation and migration of human embryonic stem cell-derived neural progenitors. *Cell Stem Cell* **6**, 323–335 (2010).
11. Shi Y, Kirwan P, Livesey FJ. Directed differentiation of human pluripotent stem cells to cerebral cortex neurons and neural networks. *Nat Protoc* **7**, 1836–1846 (2012).
12. Saatci D, van Nieuwenhuizen A, Handunnetthi L. Maternal infection in gestation increases the risk of non-affective psychosis in offspring: a meta-analysis. *J Psychiatr Res* **139**, 125–131 (2021).
13. Jiang HY, *et al.* Maternal infection during pregnancy and risk of autism spectrum disorders: A systematic review and meta-analysis. *Brain Behav Immun* **58**, 165–172 (2016).

## Figures

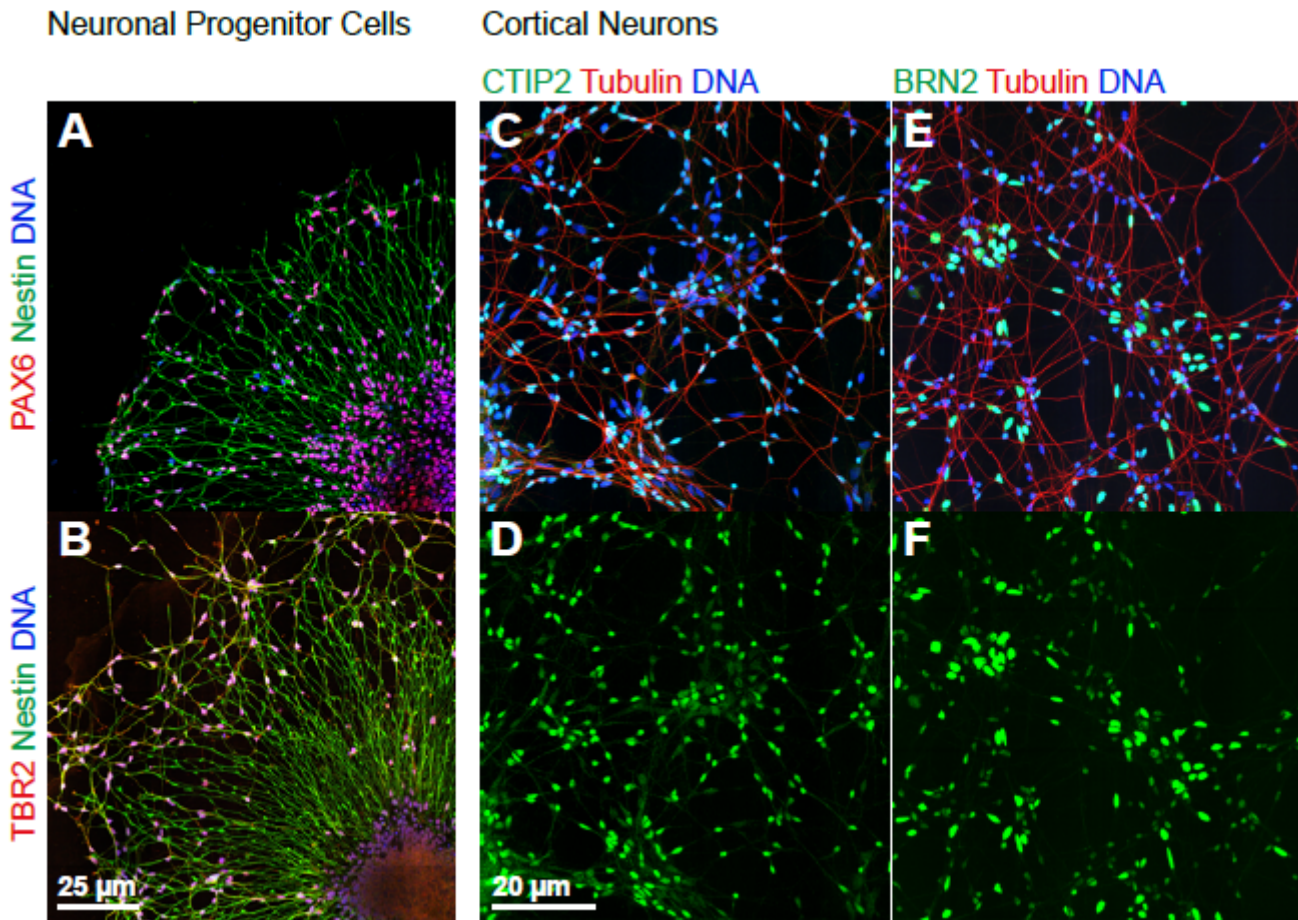


**Figure 1**

iPSC derived cortical lineage neuronal progenitor cells and cortical neurons. A: PAX6 expressing primary neuronal progenitors. B: TBR2 expressing intermediate neuronal progenitor cells. C and D: CTIP2 expressing deep cortical layer neurons. D and E: BRN2 expressing upper-layer cortical neurons.

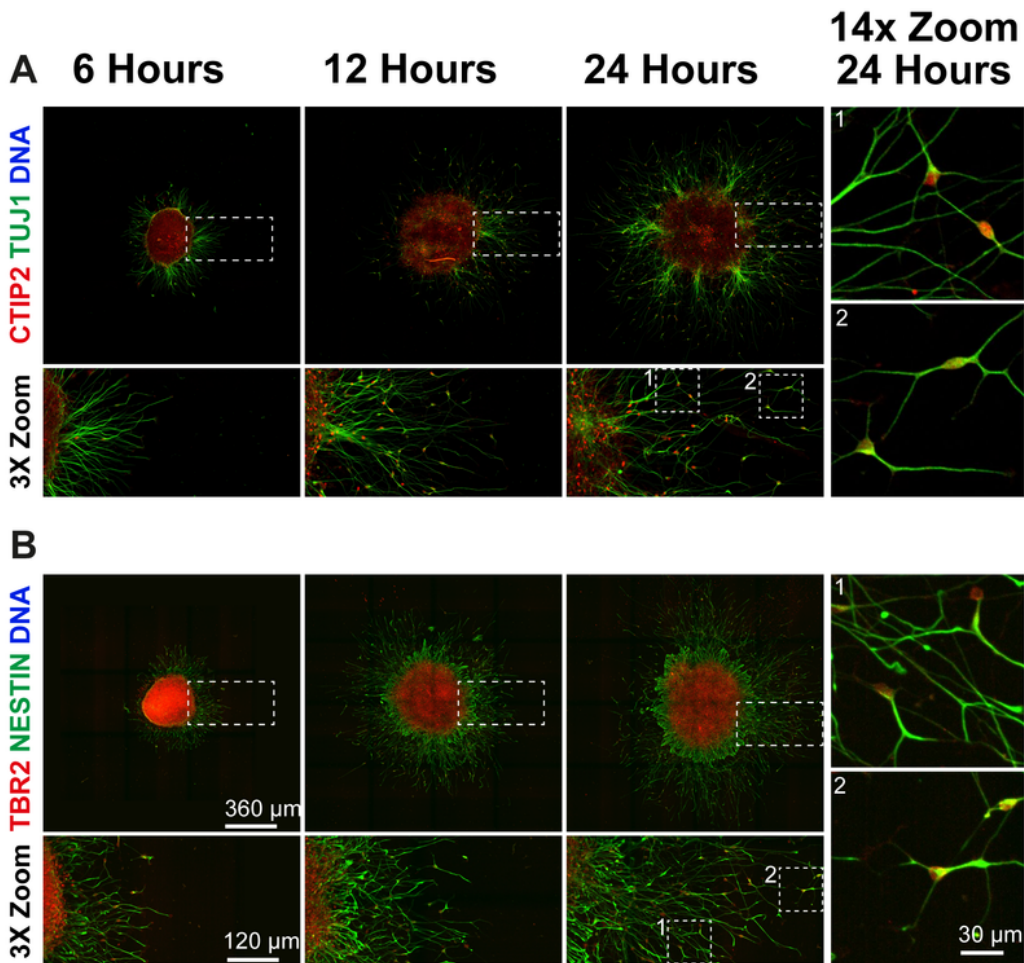


**Figure 2**

Evolution of neurospheres over three time points 6-, 12-, and 24-hours using immunofluorescence. Top panel: Appearance of CTIP2 expressing deep cortical layer neurons over time. 3X and 14X zoom panels show the migration and differentiation of CTIP2 expressing neurons as they reach the outer edge of neurospheres. Bottom panel: Appearance of TBR2 expressing intermediate neuronal progenitor cells over

time. 3X and 14X zoom panels show the appearance of TBR2 expressing intermediate neuronal progenitors within the radial extensions of neurospheres over time.

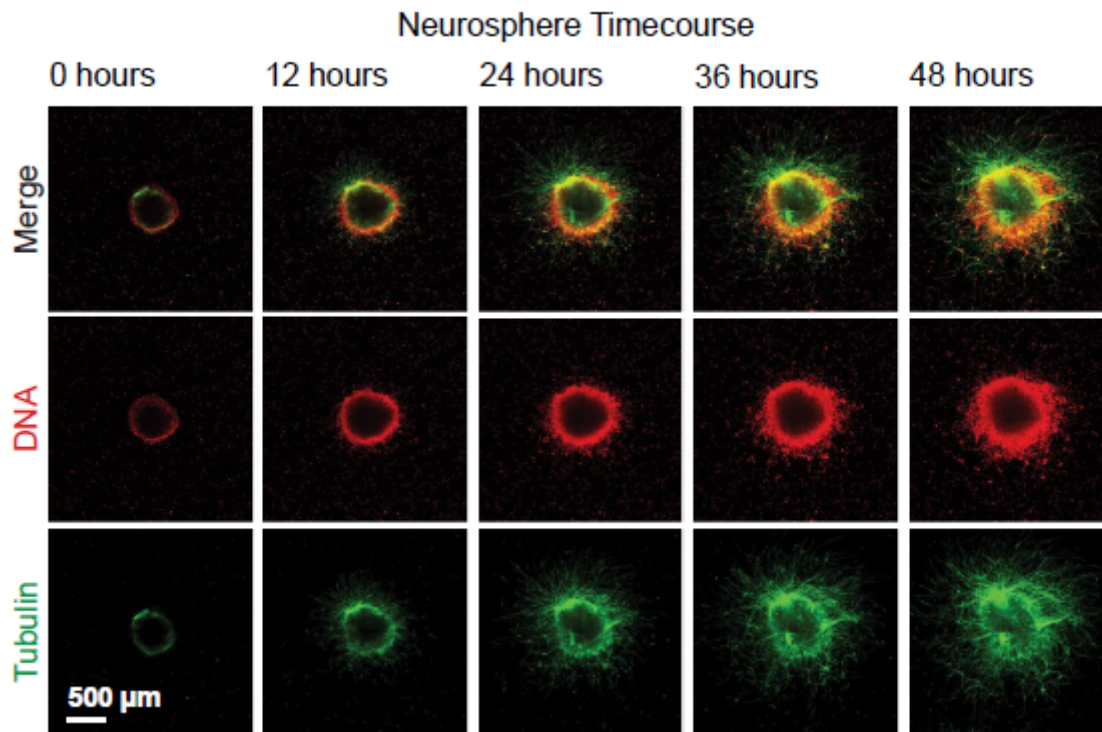


**Figure 3**

Evolution of a single neurosphere over time using live cell imaging. The top panel shows combined radial glia (Tubulin) and nuclei of migrating neural cells (DNA) at four selected time points 0, 12, 24, 36 and 48 hours. The middle and bottom panels show the breakdown of nuclei of migrating neural cells (DNA) and radial glia (Tubulin) respectively at 0, 12, 24, 36 and 48 hours. The middle and bottom panels show the breakdown of nuclei of migrating neural cells and radial glia respectively at time points 0, 12, 24, 36 and 48 hours.

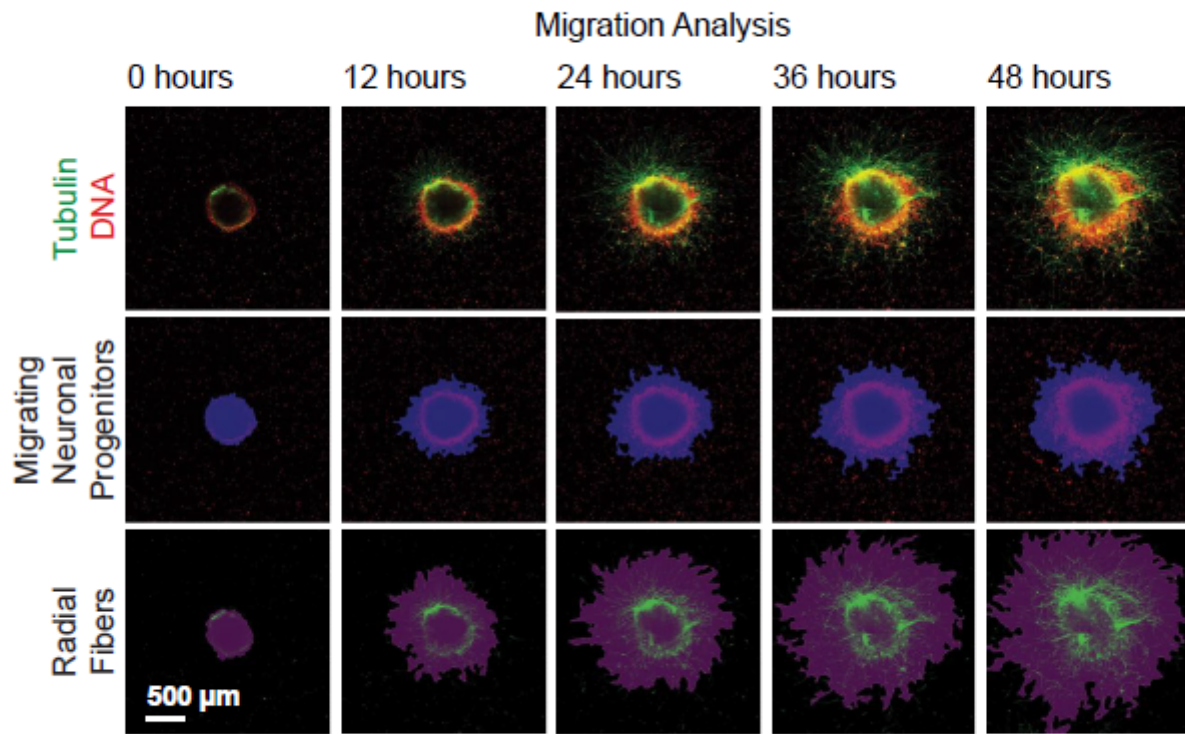


**Figure 4**

Automated analysis pipeline. Top panel shows the temporal evolution of a single neurosphere. The middle panel shows how the area of migrating neural cells is tracked over time. The bottom panel shows how the area of radial glia growth is quantified over time.

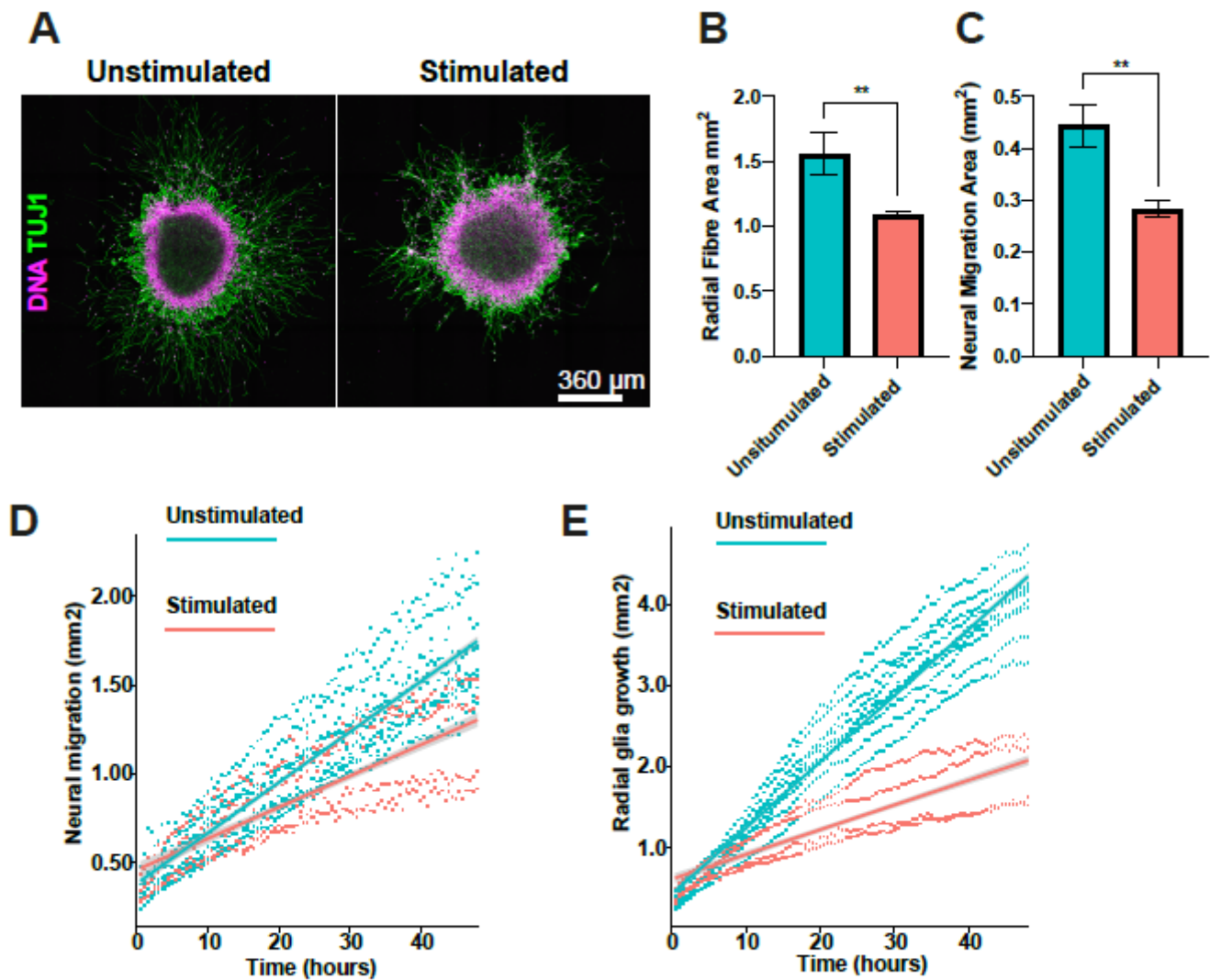


**Figure 5**

The effect of viral infection on cortical development. A: Images of fixed poly:I:C stimulated and unstimulated neurospheres after 24 hours. B and C: Analysis of immunofluorescence data from fixed neurospheres B: Comparison of radial fibre extension between poly:I:C stimulated and unstimulated neurospheres using immunofluorescence. C: Comparison of neural migration area between poly:I:C stimulated and unstimulated neurospheres using immunofluorescence. D and E: Analysis of live imaging data. D: Mixed effects linear models showing neural migration based on stimulation status over time. E: Mixed effects linear models showing radial glia extension based on stimulation status over time.

## Supplementary Files

This is a list of supplementary files associated with this preprint. Click to download.

- [supplementarymaterial.docx](#)
- [supplementarymoviecombined.mov](#)
- [supplementarymovie2radialfibres.mov](#)
- [supplementarymovie3neuralmigration.mov](#)